

A COMPILED CATALOGUE OF SPECTROSCOPICALLY DETERMINED ELEMENTAL ABUNDANCES FOR STARS WITH ACCURATE PARALLAXES. MAGNESIUM

T.V. Borkova, V.A. Marsakov

Institute of Physics, Rostov State University,
194, Stachki street, Rostov-on-Don, Russia, 344090
e-mail: borkova@ip.rsu.ru, marsakov@ip.rsu.ru

accepted 2005, Astr. Rep., v.49, No 5

Abstract

We present a compiled catalogue of effective temperatures, surface gravities, iron and magnesium abundances, distances, velocity components, and orbital elements for stars in the solar neighborhood. The atmospheric parameters and iron abundances are averages of published values derived from model synthetic spectra for a total of about 2000 values in 80 publications. Our relative magnesium abundances were found from 1412 values in 31 publications for 876 dwarfs and subgiants using a three-step iteration averaging procedure, with weights assigned to each source of data as well as to each individual determination and taking into account systematic deviations of each scale relative to the reduced mean scale. The estimated assumed completeness for data sources containing more than five stars, up to late December 2003, exceeds 90 %. For the vast majority of stars in the catalogue, the spatial-velocity components were derived from modern high-precision astrometric observations, and their Galactic orbit elements were computed using a three-component model of the Galaxy, consisting of a disk, a bulge, and a massive extended halo.

Introduction

Detailed study of the abundances of several elements in stars of various ages can be used to trace the Galaxy's chemical evolution and identify the sources in which various elements are synthesized, enabling progress in our understanding of the history of star formation and of the origin of our Galaxy's multi-component structure. According to current ideas, at least four subsystems can be identified in the Galaxy: the thin disk, thick disk, proto-disk halo, and accreted halo. It is believed that the first three subsystems formed from the same collapsing proto-galactic cloud, whereas the last subsystem was formed of isolated proto-galactic fragments and the debris of dwarf satellite galaxies that were disrupted and captured by the Galaxy at various stages of its evolution. (For more detail on the presence of accreted-halo stars in the solar vicinity, see Borkova, Marsakov (2004) and references therein.) Since the vast majority of stars in the solar neighborhood are members of the thin-disk and thick-disk subsystems, the chemical compositions of these subsystems

are best known. One striking result is that the thin-disk stars clearly exhibit a decrease in their relative abundances of α -process elements, $[\alpha/\text{Fe}]$, with increasing metallicity, $[\text{Fe}/\text{H}]$. This means that the rate of iron enrichment of the interstellar medium during the thin-disk formation stage was greater than the rate of enrichment in α -process elements. In addition, there is a strong difference between the thick-disk and thin-disk subsystems in their relative abundances of α -process elements, testifying that the transition between the two disks was discrete (see, for instance, Gratton et al., (1996), (2000), Fuhrmann (1998), (2000)). Another interesting result is the absence of appreciable differences in the $[\alpha/\text{Fe}]$ ratios for proto-disk halo and thick-disk stars. This can be interpreted as evidence that these two systems were formed during a time so short that close binaries with component masses of 4–8 M_{\odot} did not have time to evolve, explode as type Ia supernovae, and enrich the interstellar medium with iron-peak elements. The large scatter in the relative abundances of α -process elements in the halo is interpreted as evidence that mixing in the interstellar medium was weak during the formation of the halo subsystem (see, for instance, Fuhrmann (2002)). The closeness of the ages of the stars in these two subsystems has even led some authors to doubt the existence of two separate subsystems, and to suggest that the thick disk and proto-disk halo should be combined into a single subsystem (Fuhrmann (2006), Gratton et al. (2003)). Note, however, that these conclusions are based on very limited samples, with possible selection effects due to the extreme kinematic criteria used to isolate stars belonging to each of the subsystems. In fact, a more careful study of the relative abundances of α -process elements for thick-disk stars revealed a slight decrease of $[\alpha/\text{Fe}]$ with increasing metallicity, considered to be evidence for the onset of enrichment of the interstellar medium with iron by type Ia supernovae Prochaska et al. (2000). This means that the formation of the thick disk began more than ≈ 1 billion years after the first burst of star formation in the collapsing proto-Galactic cloud. It was also found that a large number of stars with ratios $[\alpha/\text{Fe}] \leq 0.25$ are observed in the range $[\text{Fe}/\text{H}] \approx -1.0 \dots -1.5$, which is more characteristic of thin-disk stars (see, for example, Nissen & Schuster (1997)). In addition, most stars with unusually low abundances of α -process elements have retrograde orbits and so were probably captured from dwarf satellite galaxies. This hypothesis is supported by the results of Shetrone et al. (2003) and Tolstou et al. (2003), who showed that stars with low $[\alpha/\text{Fe}]$ values are actually observed in dwarf spheroidal galaxies.

As we noted, the results cited above were obtained from fairly limited samples, which were often influenced by significant kinematic selection effects, and so require additional verification. The abundances of a number of elements have been published for numerous stars in the solar neighborhood. These were derived by different groups and have different accuracies. The best-studied α -process element is magnesium: unevolved F-G stars possess optical lines of this element with various intensities produced by atoms in various excited states. Accordingly, the aim of our study is to compile a uniform master catalog of relative magnesium abundances for solar-vicinity stars reduced to a unified scale using essentially all published data, along with computed spatial-velocity components and Galactic orbital elements based on accurate trigonometric parallaxes, proper motions, and radial velocities. This catalog will make it possible to extract samples in order to study various subsystems, not only with considerably larger volumes, but also largely free of artificial selection effects. Later, we will use these data together with theoretical evolutionary tracks to determine the ages of stars that have begun to leave the main sequence, taking into account the abundances of their α -process elements. The high-accuracy kinematic data of our compiled catalog will make it possible to reliably assign stars to particular subsystems of the Galaxy, and enable comprehensive statistical analyses of the stellar populations chemical, physical,

spatial, and kinematic properties. At the same time, homogeneous data on the relative magnesium abundances of stars currently in the solar vicinity but born at various distances from the Galactic center can be used to reconstruct the star-formation history and the evolution of the interstellar medium's chemical composition during the early stages of the formation of our Galaxy.

PREPARATION OF THE COMPILED CATALOGUE

The various published abundances of an element for a given star often differ quite appreciably, even when the spectra reduced by different authors are of similarly high quality. Extraction of the needed information from the spectra is based solely on current ideas concerning the structure of stellar atmospheres, and these ideas develop via the usual iterative process. It is therefore not surprising that different authors have preferred to use somewhat different theoretical model stellar atmospheres and develop different techniques for reducing and theoretically analyzing spectra. In several leading groups, analyses of spectral-line formation have been carried out without assuming local thermodynamic equilibrium. In fact, it is always necessary to analyze non-LTE effects for any abundance determinations. However, the assumption of LTE is justified for the atmospheres of dwarfs due to their high densities of particles, whose collisions bring the atomic-level populations into equilibrium. In particular, detailed computations have demonstrated that non-LTE corrections for magnesium in F-G dwarfs and subgiants are small, within 0.1 dex, and thus are smaller than the internal uncertainties in the Mg abundances Shimanskaya et al. (2000). To avoid uncertainties due to non-LTE effects for lines of iron, we always used abundances derived solely from Fe II lines. (Note that, in his determinations of relative stellar magnesium abundances assuming LTE, Fuhrmann (1998), (2000) used lines of neutral elements for which the non-LTE effects are approximately the same, and his resulting [Mg I/Fe I] ratios are nearly unbiased.)

These factors explain the reasons for the deviations among the data obtained and analyzed by different authors. We also cannot rule out the possibility of systematic differences between the magnesium abundances presented in different papers. If several abundance values are available for the same star, they can simply be averaged. However, when an abundance is presented in only one paper, the possibility of systematic differences must be considered. We collected all available lists (with ≥ 5 stars) of relative magnesium abundance estimates, [Mg/Fe], for field stars from high-resolution spectra with high signal-to-noise ratios published after 1989. We estimate the completeness of the abundances published for solarvicinity stars up through December 2003 to be better than 90 %. The largest of the source catalogs contain only about 200 stars (Table 1). Note that our aim is not to analyze the origin of discrepancies among the data, but to compile a list of published spectroscopic relative magnesium abundances for field stars that is as complete as possible, and is reduced to a uniform scale. The raw material for this study were 36 publications containing 1809 magnesium-abundance determinations for 1027 stars. Of these stars, we retained only 876 dwarf and subdwarf stars that lie below the solid line in the Hertzsprung-Russell diagram in Fig. 1a. This line was plotted by eye, parallel to the zero-age main sequence, to exclude stars in more advanced evolutionary stages. This automatically rejected five publications in which only giants had been studied.

Table 1: The weights, p_j , and systematic deviations, $\Delta[\text{Mg}/\text{Fe}]_j$, derived for each of the lists in two metallicity ranges

Data source	Total number of stars	[Fe/H]≤-1.0			[Fe/H]>-1.0		
		$\Delta[\text{Mg}/\text{Fe}]_j$	p_j	N	$\Delta[\text{Mg}/\text{Fe}]_j$	p_j	N
Edvardsson et al. (1993)	178	–	–	–	-0.045	1.00	167
Nissen & Schuster (1997)	30	+0.001	1.00	7	+0.046	0.60	22
Mashonkina et al. (2003)	61	-0.056	0.64	27	-0.026	0.63	32
(2000)	15	+0.034	1.00	13	-0.069	0.63	2
Fuhrmann (1998, 2000)	111	-0.040	0.52	6	+0.006	0.81	76
Fuhrmann (1995)	52	+0.053	0.60	20	+0.053	0.63	22
Chen et al. (2000, 2003)	93	–	–	–	-0.011	0.64	59
Mishenina (2001, 2004)	209	+0.070	0.67	21	+0.004	0.69	77
Clementini et al. (1999)	16	-0.0035	0.61	7	+0.041	0.49	7
Carretta et al. (2000)	9	–	–	–	+0.008	0.70	5
Nissen (1994)	8	-0.030	0.96	7	–	–	–
Gehren (1998, 2000, 2004)	51	-0.019	0.57	16	+0.011	0.46	21
Magain (1989)	20	-0.111	0.43	20	–	–	–
Jehin et al. (1999)	20	–	–	–	+0.017	1.00	20
Stephens (1999, 2002)	55	-0.082	0.28	8	–	–	–
Carney et al. (1997)	7	-0.050	0.63	7	–	–	–
Idiart et. al. (1999)	217	+0.129	0.40	40	+0.052	0.80	176
Procheska et al. (2000)	10	–	–	–	+0.040	1.00	8
Bensby et al. (2003)	65	–	–	–	-0.002	0.66	27
(2002)	20	+0.098	0.33	11	-0.080	0.76	4
Rayn et al. (1991, 1996)	27	-0.030	0.33	9	–	–	–
Gratton et al. (2003)	142	-0.077	0.67	41	-0.076	0.77	53
Reddy et al. (2003)	176	–	–	–	+0.046	0.90	30

Note. The "N" columns give the number of a list's stars that are also present in other sources

Atmospheric Parameters and Iron Abundances

Atmospheric Parameters and Iron Abundances We simply averaged the stellar effective temperatures and surface gravities from the cited papers, in which these parameters were determined using various methods. For both parameters, we estimated the uncertainties of the averages based on the scatter of the individual values about the average for each star; i. e., from the agreement of the values obtained by the various authors. For this purpose, we calculated the deviations $dX_i = \langle X \rangle - X_i$ for stars for which these parameters were determined in several studies, where the index i refers to the individual measurements for a given star. Note that our uncertainty estimates are based on as many as 80 publications, since we also used here studies devoted to spectroscopic abundance determinations for other elements (see the numbers of stars in the histograms, Fig. 2). We then plotted the corresponding distributions and calculated the dispersions of Gaussian curves describing them, which were equal to $\varepsilon(T_{\text{eff}}) = \pm 56 \text{ K}$ and $\pm 82 \text{ K}$ and $\varepsilon(\log g) = \pm 0.12$ and ± 0.24 for stars with $[\text{Fe}/\text{H}]$ values above and below -1.0 , respectively. The good agreement of the observed distributions with the Gaussian curves shows that the deviations are random, so that their dispersions should reflect the actual uncertainties in the parameters. Our $[\text{Fe}/\text{H}]$ values for each star are also averages of metallicities from the same papers, with uncertainties estimated as $\varepsilon([\text{Fe}/\text{H}]) = \pm 0.07 \text{ dex}$ and $\pm 0.13 \text{ dex}$, respectively, for metal-rich and metal-poor stars. All these estimates are close to the lower limits of the uncertainties for these parameters claimed by the authors. These distributions and the approximating normal curves are displayed in Fig. 2. We found it necessary to differentiate between the two metallicity groups because the uncertainties in all the parameters are considerably larger for the metal-poor stars.

Iterative Procedure Used to Calculate the Relative Magnesium Abundances

To get an idea of the number of abundance determinations for the individual stars, see the histogram in Fig. 1b, which presents the distribution of the number of sources for the stars. This histogram shows that the number of stars decreases exponentially with increasing number of magnesium-abundance determinations, so that only single determinations are available for more than half the stars in the sample. To derive reliable abundances, we applied a somewhat modified version of the three-step iterative technique for compiling data presented by Castro et al. (1997).

Figure 3 presents several diagrams that compare the $[\text{Mg}/\text{Fe}]$ ratios for the lists having the largest numbers of stars in common. We can see that the values of all the authors are fairly well correlated, with all the correlation coefficients being $r \geq 0.8$. However, small (within the uncertainties) systematic deviations are present in the data. Not only are the results of the LTE and non-LTE approximations different, but there exist discrepancies within each of these approximations. In particular, the two diagrams in the upper panel of Fig. 3 demonstrate the scatter of the estimates obtained using a single approximation. The two diagrams in the middle panel, which compare the abundances derived using different approximations, show only scatter without a considerable systematic offset. On the other hand, appreciable systematic differences can appear not only between the values obtained using different approximations, but also between the values obtained by different authors using the same approach (Figs. 3e and 3f). If there are no regular systematic differences related to a particular approach, we can simply average all these data for each star.

After averaging (calculating the individual preliminary mean values, $\langle [\text{Mg}/\text{Fe}]_i \rangle$), we can check whether the systematic differences and scatter of the $[\text{Mg}/\text{Fe}]_i$ values for different authors depend on metallicity. Figure 4 shows the relations between the deviations $\delta [\text{Mg}/\text{Fe}]_i = \langle [\text{Mg}/\text{Fe}]_i \rangle - [\text{Mg}/\text{Fe}]_i$ and $[\text{Fe}/\text{H}]_i$ for some of our lists. The subscript i here refers to an individual abundance determination for a star. The diagrams demonstrate that the scatter of the deviations and the systematic offset of $\delta [\text{Mg}/\text{Fe}]_i$ relative to the mean (zero) vary from list to list and also depend on metallicity. Sometimes the scatter and systematic offset remain practically the same over the whole metallicity range (Figs. 4a and 4b). Weak trends with various signs are common. The $\delta [\text{Mg}/\text{Fe}]_i$ deviations sometimes move upwards (Figs. 4c and 4d) and sometimes downwards (Figs. 4e and 4f) with increasing metallicity in the diagram. To take these small but systematic trends into account, we divided each list into two metallicity magnesium-ranges at $[\text{Fe}/\text{H}] = -1.0$ and calculated the mean deviations for these ranges; i. e., the systematic deviations $\Delta [\text{Mg}/\text{Fe}]_i = \langle \delta [\text{Mg}/\text{Fe}]_j \rangle$ (see the dotted lines in the diagrams). We then corrected all the individual $[\text{Mg}/\text{Fe}]_i$ values for these biases. As noted above, these corrections leave the magnesium abundances for stars present in several lists virtually unchanged. However, if a star's magnesium abundance was determined in a single study only, the correction will strongly affect the final magnesium abundance. Indirect confirmation that it is appropriate to correct for these systematic differences is provided by the fact that the scatter of the data points in the final $[\text{Fe}/\text{H}]-[\text{Mg}/\text{Fe}]$ diagram plotted for the sample stars became considerably smaller after applying the corrections, and characteristic features observed in the data for individual sources became more prominent (compare Fig. 10 below and Fig. 6 in Mashonkina et al. (2003)).

The next step after correcting for systematic biases was to determine weights for the data sources in the lists and calculate new weighted means. Figures 3 and 4 show that the scatters in the diagrams - i. e., the $[\text{Mg}/\text{Fe}]$ uncertainties in the lists - are not all the same. Accordingly, each list was assigned a weight that was inversely proportional to the corresponding dispersion for the deviations in each of the metallicity ranges. The lowest scatter for the higher metallicities was found for the lists of Prochaska et al. (2000), Edvardsson et al. (1993), Jehin et al. (1999), and they were assigned unit weights. At lower metallicities, the lowest scatter was shown by the lists of Nissen & Schuster (1997), Mashonkina et al. (2003). The lowest weights assigned to some of the lists were ≈ 0.3 . The weights and biases for each list in each of the two metallicity ranges are collected in Table 1. We then calculated a new weighted mean magnesium abundance for each star taking into account the biases and weights assigned to the lists.

Let us briefly discuss one important aspect of compiling the data. In practice, small catalogs can have few stars in common even with the largest original catalogs. Thus, to analyze the agreement between their values and the values of other authors and assign them correct weights, we combined the small catalogs into larger lists, each containing a series of studies by the same group in which the same techniques were used to derive the abundances. For lists containing several values for the same star, we chose the more recent values. As a result, we obtained 24 lists including 31 primary data sources (Table 2¹). Further, all the lists were used to calculate preliminary mean magnesium abundances for each star in the sample. (The only exception was Castro et al. (1997): none of its nine stars were found in any other source, and all the data for these stars were entered into the final catalog without any changes.)

¹Table 2 of this paper is presented only electronically and can be found at <http://cdsweb.u-strasbg.fr/cats/J.AZh.htm>. A description of this table is given in the Appendix.

The next step was also a weight-assigning procedure, this time for individual values, $[\text{Mg}/\text{Fe}]_{ij}$, where the first subscript refers to the value and the second to the list. This procedure was intended to assign lower weights to initial values showing larger deviations. Clearly, such a procedure can work only if there are three or more values for the same star. This step makes use of the deviations from the calculated weighted means, δ_{ij} , for individual values (with their biases taken into account). When assigning the weights p_{ij} , we considered the mean absolute value, ε_j , of the deviations for all stars in the list containing the given value. The weights were calculated using the formula $p_{ij} = \sqrt{2\varepsilon_j^2 / (\delta_{ij}^2 + \varepsilon_j^2)}$. We can see that an individual weight of unity was assigned to values whose deviations were equal to the mean deviation. Most stars in the list were given weights slightly greater than unity, $(p_{ij})_{\text{max}} = \sqrt{2}$. However, the weights begin to decrease appreciably for $\delta_{ij} > \varepsilon_j$.

As a result, this procedure assigns the lowest weights to the least-reliable determinations and enables us to obtain final values that are close to those given for most of the sources, with no single measurement rejected. Some idea of the internal accuracy of our final $[\text{Mg}/\text{Fe}]$ values can be obtained from the dispersion of the distribution of all the deviations δ_{ij} , equal to $\varepsilon [\text{Mg}/\text{Fe}] = 0.05$ and 0.07 dex for metal-rich and metal-poor stars, respectively (Fig. 5). The final weighted mean $[\text{Mg}/\text{Fe}]$ values calculated for our sample of dwarfs and subgiants in the solar neighborhood are presented in Table (see the Appendix).

Distances, Proper Motions, and Radial Velocities

We determined the distances to the stars using trigonometric parallaxes with uncertainties below 25 % from the catalogs Hipparcos (1997), Kharchenko (2001), Myers et al. (2002) or, in their absence, we adopted the photometric distances from the catalogs Carney et al. (1994), Nordstrom et al. (2004), derived using $\text{uvby}\beta$ photometric data. The uncertainty in photometric distances is usually claimed to be ± 13 % Nordsrom et al. (2004). Figure 6 shows the distribution of the distances of the sample stars from the Sun. The distributions ascending branch lasts only to 5 pc, after which a steep decline begins, testifying that most of the sample stars are close to the Sun. The photometric distances were used only for the most distant stars.

We took the proper motions from the catalogs Hipparcos (1997), Kharchenko (2001), Myers et al. (2002), Beer et al. (2000), Carney et al. (1994), Bakos et al. (2002) the order of the catalogues corresponds to priority of utilizations). For most stars in our sample, the typical uncertainties in their proper motions are ≈ 1.8 milliarcseconds/year, corresponding to a mean uncertainty in the tangential velocity of $\approx \pm 0.8$ km/s.

We took the radial velocities from the catalogs Nidever et al. (2002), Barbier-Brossat & Figon (2000), Barbier-Brossat et al. (2002), Nordstrom et al. (2004) the order of the catalogues corresponds to priority of utilizations). If the required data were not present in any of these catalogs, we took them from other publications (see references to Table in the Appendix). The characteristic uncertainties in the radial velocity measurements for the sample stars are $\approx \pm 0.6$ km/s (Myers et al. (2002)).

Spatial Velocities and Galactic Orbital Elements

Spatial Velocities and Galactic Orbital Elements We computed the U , V , and W components of the total spatial velocity relative to the Sun for 850 stars with distances, proper motions, and radial velocities (U is directed towards the Galactic anticenter, V in the

direction of the Galactic rotation, and W toward the North Galactic pole). The main contribution to the uncertainties in the spatial velocities comes from the uncertainties in the distances, rather than the uncertainties in the tangential and radial velocities. For mean distance uncertainties of 15 % and the mean distance from the Sun of the sample stars, ≈ 60 pc, the mean uncertainty in the spatial velocity components is $\approx \pm 2$ km/s.

We adopted a Galactocentric distance for the Sun of 8.5 kpc, a rotational velocity for the Galaxy at the solar Galactocentric distance of 220 km/s, and a velocity for the Sun relative to the Local Standard of Rest of $(U_\odot, V_\odot, W_\odot) = (-11, 14, 7.5)$ km/s Ratnatunga et al. (1989). We used these values to calculate the components of the spatial velocities in cylindrical coordinates, (Θ, Π, W) , and the total residual velocities of the stars relative to the Local Standards of Rest, V_{res} .

We calculated the Galactic orbital elements by modeling 30 orbits of each star around the Galactic center using the multi-component model for the Galaxy of Allen & Santillan (1991), which consists of a disk, bulge, and extended massive halo.

A list of the stars with all the parameters described in this paper is presented in Table 2 (see its description in the Appendix). The catalog itself is published only electronically, at the address <http://cdsweb.u-strasbg.fr/cats/J.AZh.HTX>

ANALYSIS OF THE SAMPLE

All the published catalogs can be tentatively subdivided into two groups based on the principle applied to select stars for spectroscopic determinations of the abundances of various elements. The first group consists of various samples whose stars were selected based on a limiting apparent magnitude. Since the Sun is situated near the Galactic plane, such samples contain almost exclusively stars of the disk subsystems, with very few halo (i.e., low-metallicity) stars. Thus, a preliminary selection of low-metallicity stars using photometric data is needed for spectroscopic observations of objects in the halo subsystems. The apparent magnitudes of the stars selected in this way are much fainter. This is clearly illustrated in the $[\text{Fe}/\text{H}]-\text{V}$ diagram for our sample stars (Fig. 7). Nearly all the stars with $[\text{Fe}/\text{H}] \geq -1.0$ are brighter than $\text{V} \approx 9^m$, whereas most of the more metal-poor stars are fainter. The stars of both groups cover the sky rather uniformly, with an understandable concentration of metal-richer stars toward the Galactic plane (Fig. 8). This observational selection effect should be born in mind when estimating the relative numbers of stars of various metallicities in the solar neighborhood. Figure 9 displays the $[\text{Fe}/\text{H}]$ and $[\text{Mg}/\text{Fe}]$ distributions for the resulting sample, while Fig. 10 shows the corresponding $[\text{Fe}/\text{H}]-[\text{Mg}/\text{Fe}]$ diagram.

We are preparing a cycle of papers in which we identify stars belonging to the thin-disk and thick-disk subsystems, as well as to the proto-disk and "accreted" halo subsystems, based on the elements of the Galactic orbits from the catalog. In these forthcoming papers, we will estimate the star-formation rates and efficiencies of mixing of the interstellar medium in the early stages of the Galaxy's evolution based on an analysis of the scatter of the relative magnesium abundances for low-metallicity stars of the old Galactic subsystems.

We are also planning to present similarly unified abundance determinations for other α -process elements in a future version of our catalog.

ACKNOWLEDGMENTS: The authors are grateful to L.I.Mashonkina for fruitful discussions of the results.

Appendix

The description of Table 2 (this Table is being published only electronically, at the address
<http://cdsweb.u-strasbg.fr/cats/J.AZh.htm>):

- (1) HD: No. in the HD catalogue { III/135 }
- (2) DM: DM number {I/119}, {I/122}
- (3) HIP: No. in the Hipparcos catalogue {I/239}
- (4) SAO: No. in the SAO catalogue {I/131}
- (5) OtherName: Other name
- (6) Vmag: Apparent V magnitude in the Johnson system
- (6) Radeg: α in degrees (ICRS, epoch J1991.25)
- (7) Dedeg: δ in degrees (ICRS, epoch J1991.25)
- (8) Plx: Trigonometric or photometric parallax

Remark to column 8:

Errors are given for trigonometric parallaxes only.

- (9) pmRA: Proper motion, $\mu_\alpha \cos \delta$
- (10) pmDE: Proper motion, μ_δ
- (11) e_Plx: Standard error of the trigonometric parallax
- (12) e_pmRA: Standard error of $\mu_\alpha \cos \delta$
- (13) e_pmDE: Standard error of μ_δ
- (14) f(pi): Data source for the star's parallax and proper motion

Remark to column 14:

The following notation is used for the references: [HIP]: The Hipparcos and Tycho Catalogues, ESO, 1997

[KHR]: Kharchenko N.V., 2001, All-sky Compiled Catalogue of 2.5 million stars, KFNT, 17, 409

[SKY]: Myers J.R., Sande C.B., Miller A.C., et al., 2002, Sky2000. Catalogue, version 4

[BCY]: Beer T.C., Chiba M., Yoshi Y., et al., 2000, Astron J., 119, 2866

[CLL]: Carney B.W., Latham D.W., Laird J.B., Aguilar L.A., 1994, Astron. J., 107, 2240

[BSN]: Bakos G.A., Sahu K.C., Nemeth P., 2002, Astrophys. J. Suppl. Ser. JS, 141, 187.

- (15) RV: Radial velocity
- (16) f(vr): Data source for the radial velocity (3)

Remark to column 16:

The following notation is used for the references:

[BBF]: Barbier-Brossat M. and Figon P., Astron. and Astrophys. 142, 217, 2000

[BG]: Barbier-Brossat M. and Gratton R.G., Astron. and Astrophys., 384, 879, 2002

[MLG]: Malaroda S., Levato H., Galliani S., Stellar Radial Velocities 1991–1998

[NMB]: Nidever D.L., Marcy G.W., Butler R.P., et al. Astron. J. Suppl. Ser., 141, 503 (2002)

[NMA]: Nordstrom B., Mayor M., Andersen J., et al., Astron. and Astrophys., 418, 989 (2004)

[MON]: Montes D., Lopez-Santiago J., Galvez M.C., et al., Monthly Notices Roy. Astron. Soc., 328, 45 (2001)

[FUL]: Fulbright J.P., Astron. J., 123, 404 (2002)
 [WBS]: Wilhelm R., Beers T.C., Sommer-Larsen J., et al., Astron. J., 117, 1229 (1999)
 [SWG]: Strassmeier K.G., Washuettl A., Granzer T., et al., Astron. and Astrophys. Suppl. Ser., 142, 275 (2000)
 [LST]: Latham D.W., Stefanik R.P., Torres G., et al., Astron. J., 124, 1144 (2002)
 [NS]: Nissen P.E., Schuster W.J. Astron. and Astrophys., 326, 751 (1997)
 [GBR]: Grenier S., Baylac M.O., Rolland L., et al., Astron. and Astrophys. Suppl. Ser., 137, 451 (1999)
 [AFG]: Axer M., Fuhrmann K., Gehren T., Astron. and Astrophys., 300, 751 (1995).

(17) Teff: Effective temperature
 (18) log g: The star's surface gravity
 (19) [Fe/H]: The star's iron abundance (4)
 (20) [Mg/Fe]: The star's magnesium-to-iron abundance

Remark to columns 19, 20:

Abundances of chemical elements are given in the logarithmic scale, expressed in solar units.

(21) f(mg): Number of data sources for [Mg/Fe]
 (22) f(sum): The data sources' combined weight

Remark to column 22:

The combined weight includes the weight of the data source (Table 1) and of the individual value (see the text).

(23) l: Galactic longitude
 (24) b: Galactic latitude
 (25) Mv: Absolute magnitude
 (26) rsun: Distance from the Sun
 (27–29) Xg, Yg, Zg: Coordinates in the galactic coordinate system
 (30) R: Distance to the star from the Galaxy's center
 (31–33) U, V, W: The stars space velocity components (see the text)
 (34, 35) Vpi, Vtet: Components of the space velocity in the cylindrical coordinate system
 (36) Vpec: The stars total peculiar velocity with respect of the Local Standard of Rest
 (37–39) Rpe, Rap, e: The stars orbital perigalactic and apogalactic radius and orbital eccentricity
 (40) Ψ : Inclination of the star's galactic orbit
 (41) Zmax: Maximal distance of the star's orbit from the galactic plane.

References

- [1.] T. V. Borkova, V. A. Marsakov, *Astronomy Letter*, **30**, 148 (2004)
- [2.] R. G. Gratton, E. Carretta, F. Matteuchi, and C. Sneden, in *Formation of the Galactic Halo Inside and Out*, ASP Conf. Ser., (eds H. Morrison and A. Sarajedini, 1996), **92**, p. 307.
- [3.] R. G. Gratton, E. Carretta, F. Matteucci, and C. Sneden, *Astron. and Astrophys.* **358**, 671 (2000).
- [4] K. Fuhrmann, *Astron. and Astrophys.* **338**, 161 (1998).
- [5] K. Fuhrmann, 2000, preprint *Nearby stars of the Galactic disk and halo. II.* Munich.
- [6] K. Fuhrmann, *New Astron.* **7**, 161 (2002).
- [7] R. G. Gratton, E. Carretta, S. Desidera, *et al.*, *Astron. and Astrophys.* **406**, 131 (2003).
- [8] J. Prochaska, S. O. Naumov, B. W. Carney, *et al.*, *Astron. J.* **120**, 2513 (2000).
- [9] P. E. Nissen and W. J. Schuster, *Astron. and Astrophys.* **326**, 751 (1997).
- [10] M. Shetrone, K. A. Venn, E. Tolstou, *et al.*, *Astron. J.* **125**, 684 (2003).
- [11] E. Tolstou, K. A. Venn, M. Shetrone, *et al.*, *Astron. J.* **125**, 707 (2003).
- [12] N. N. Shimanskaya, L. I. Mashonkina, N. A. Sakhibullin *Astron. Rep.* **44**, 530 (2000)
- [13] B. Edvardsson, J. Andersen, B. Gustafsson, *et al.*, *Astron. and Astrophys.* **275**, 101 (1993).
- [14] N. N. Shimanskaya, L. I. Mashonkina, *Astron. Rep.* **45**, 100 (2001)
- [15] L. Mashonkina, T. Gehren, C. Travaglio, and T. Borkova, *Astron. and Astrophys.* **397**, 275 (2003).
- [16] K. Fuhrmann, M. Axer, and T. Gehren, *Astron. and Astrophys.* **301**, 492 (1995).
- [17] Y. Q. Chen, P. E. Nissen, G. Zhao, *et al.*, *Astron. and Astrophys. Suppl. Ser.* **141**, 491 (2000).
- [18] Y. Q. Chen, G. Zhao, P. E. Nissen, *et al.*, *Astron. and Astrophys.* **591**, 925 (2003).
- [19] T. V. Mishenina and V. V. Kovtyukh, *Astron. and Astrophys.* **370**, 951 (2001).
- [20] T. V. Mishenina, ' Soubiran, V. V. Kovtyukh, S. A. Korotin, *Astron. and Astrophys.* **418**, 551 (2004).
- [21] G. Clementini, R. Gratton, E. Carretta, and C. Sneden, *Monthly Not. Astron. Soc.* **302**, 22 (1999).
- [22] E. Carretta, R. Gratton, and C. Sneden, *Astron. and Astrophys.* **356**, 238 (2000).
- [23] P. E. Nissen, B. Gustafsson, B. Edvardsson, and G. Gilmore, *Astron. and Astrophys.* **440** (1994).

[24] R. Ottmann, M. J. Pfeiffer, and T. Gehren, *Astron. and Astrophys.* **338**, 661 (1998).

[24] G. Zhao and T. Gehren, *Astron. and Astrophys.* **362**, 1077 (2000).

[26] T. Gehren, Y. C. Liang, J. R. Shi, *et al.*, *Astron. and Astrophys.* **413**, 1045 (2004).

[27] P. Magain, *Astron. and Astrophys.* **209**, 211 (1989).

[28] E. Jehin, P. Magain, C. Neuforge, *et al.*, *Astron. and Astrophys.* **341**, 241 (1999).

[29] A. Stephens, *Astron. J.* **117**, 1771 (1999).

[30] A. Stephens and A. M. Boesgaard, *Astron. J.* **123**, 1647 (2002).

[31] B. W. Carney, J. S. Wright, C. Sneden, *et al.*, *Astron. J.* **114**, 363 (1997).

[32] T. Idiart and F. Thevenin, *Astrophys. J.* **541**, 207 (2000).

[33] T. Bensby, S. Feltzing, and I. Lundstrom, *Astron. and Astrophys.* **410**, 527 (2003).

[34] S. V. Ermakov, Ph. dissertation in Mathematical Physics (SAO, 2002)

[35] S. G. Ryan, J. E. Norris, and M. S. Bessell, *Astron. J.* **102**, 303 (1991).

[36] S. G. Ryan, J. E. Norris, and T. C. Beers, *Astrophys. J.* **471**, 254 (1996).

[37] R. Gratton, E. Carretta, R. Claudi, *et al.*, *Astron. and Astrophys.* **404**, 187 (2003).

[38] B. E. Reddy, J. Tomkin, L. Lambert, *et al.*, *Monthly Not. Astron. Soc.* **340**, 304 (2003).

[39] B. Hauck and M. Mermilliod, *Astron. and Astrophys. Suppl. Ser.* **129**, 431 (1998).

[40] S. Castro, R. M. Rich, M. Grenon, *et al.*, *Astron. J.* **114**, 376 (1997).

[41] The Hipparcos and Tycho Catalogues, ESO, 1997.

[42] N. V. Kharchenko, All-sky Compiled Catalogue of 2.5 million stars, *KFNT* **17**, 409 (2001).

[43] J. R. Myers, C. B. Sande, A. C. Miller, Jr. W. H. Warren, and D. A. Tracewell, 2002, Sky2000 Catalogue, version 4.

[44] B. W. Carney, D. W. Latham, J. B. Laird, and L. A. Aguilar, *Astron. J.* **107**, 2240 (1994).

[45] B. Nordstrom, M. Mayor, J. Andersen, *et al.*, *Astron. and Astrophys.* **418**, 989 (2004).

[46] T. C. Beer, M. Chiba, Y. Yoshi, *et al.*, *Astron. J.* **119**, 2866 (2000).

[47] G. A. Bakos, K. C. Sahu, and P. Nemeth, *Astrophys. J. Suppl. Ser.* **141**, 187 (2002).

[48] D. L. Nidever, G. W. Marcy, R. P. Butler, D. A. Fischer, and S. S. Vogt, *Astrophys. J. Suppl. Ser.* **141**, 503 (2002).

[49] M. Barbier-Brossat and P. Figon, *Astron. and Astrophys.* **142**, 217 (2000).

[50] M. Barberi and R. G. Gratton, *Astron. and Astrophys.* **384**, 879 (2002).

- [51] K. U. Ratnatunga, J. N. Bahcall, and S. Casrtano, *Astrophys. J.* **291**, 260 (1989).
- [52] C. Allen and A. Santillan, *Rev. Mex. Astron. y Astrofis.* **22**, 255 (1991).

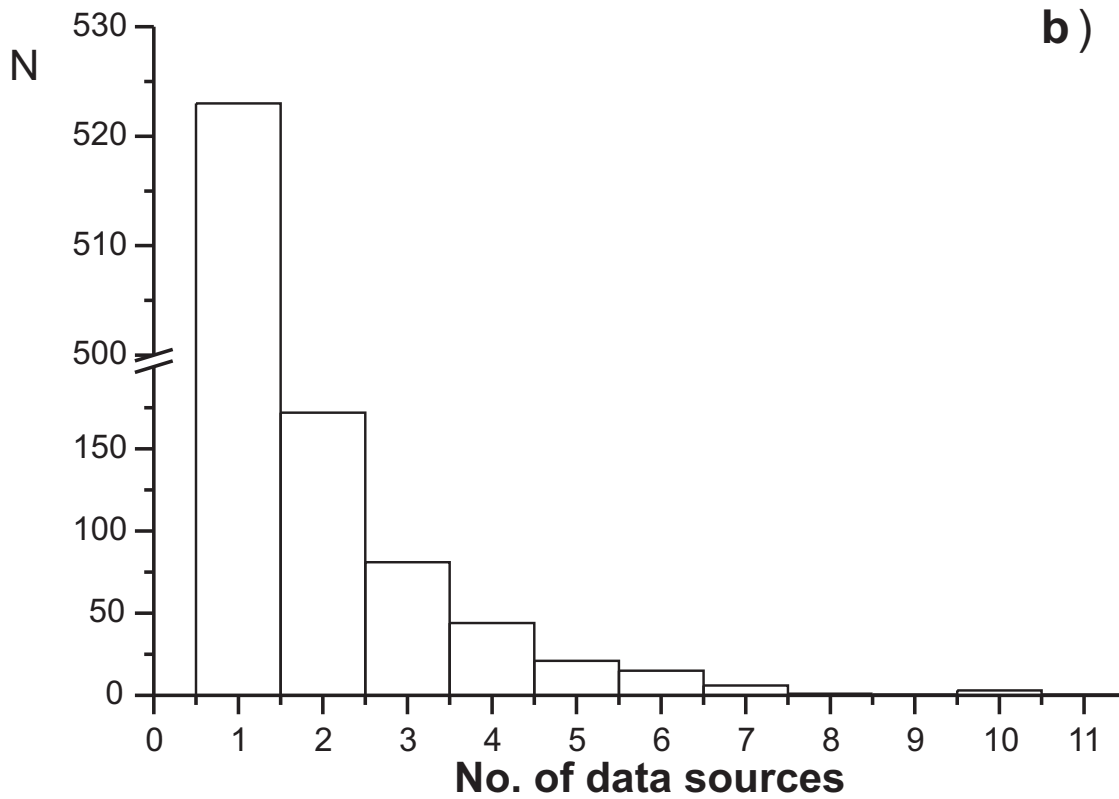
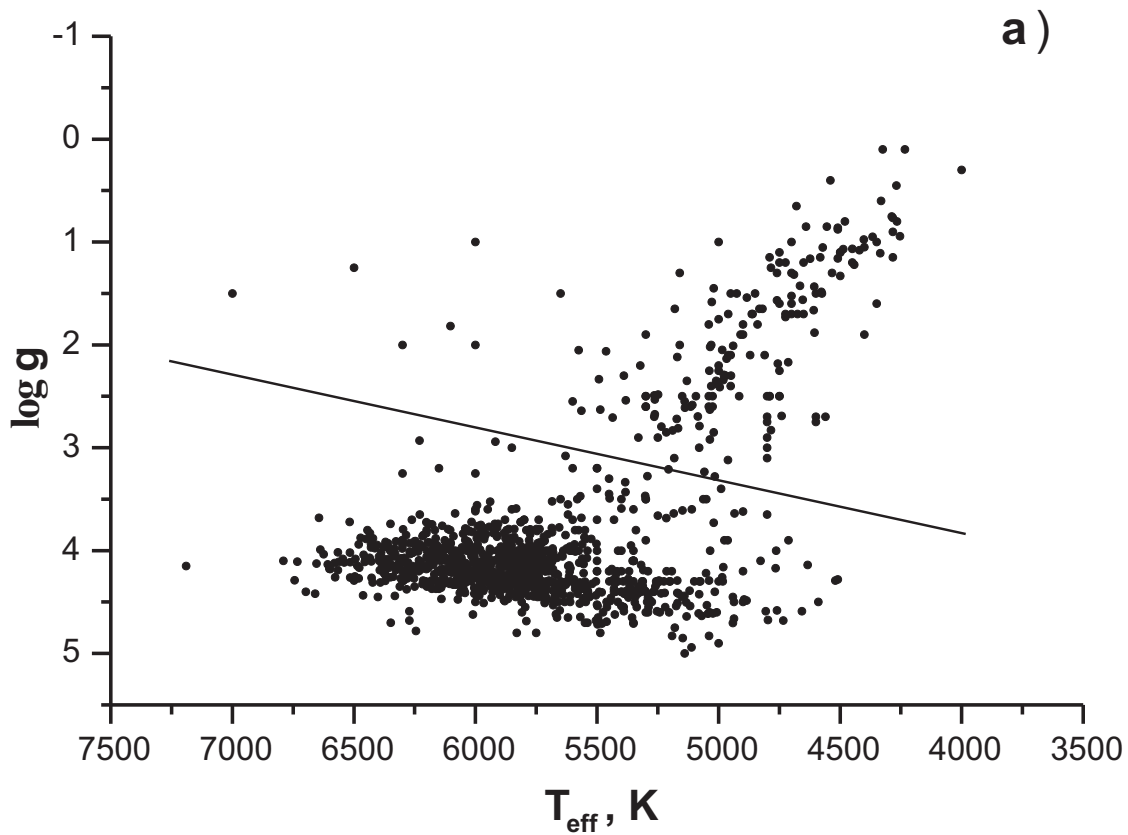


Figure 1: The T_{eff} – $\log g$ diagram for stars with magnesium abundances found in the literature (a) and the stars' distribution over the number of magnesium-abundance determinations available for them (b). Only stars that lie below the sloping line in the diagram (a) enter our catalogue.

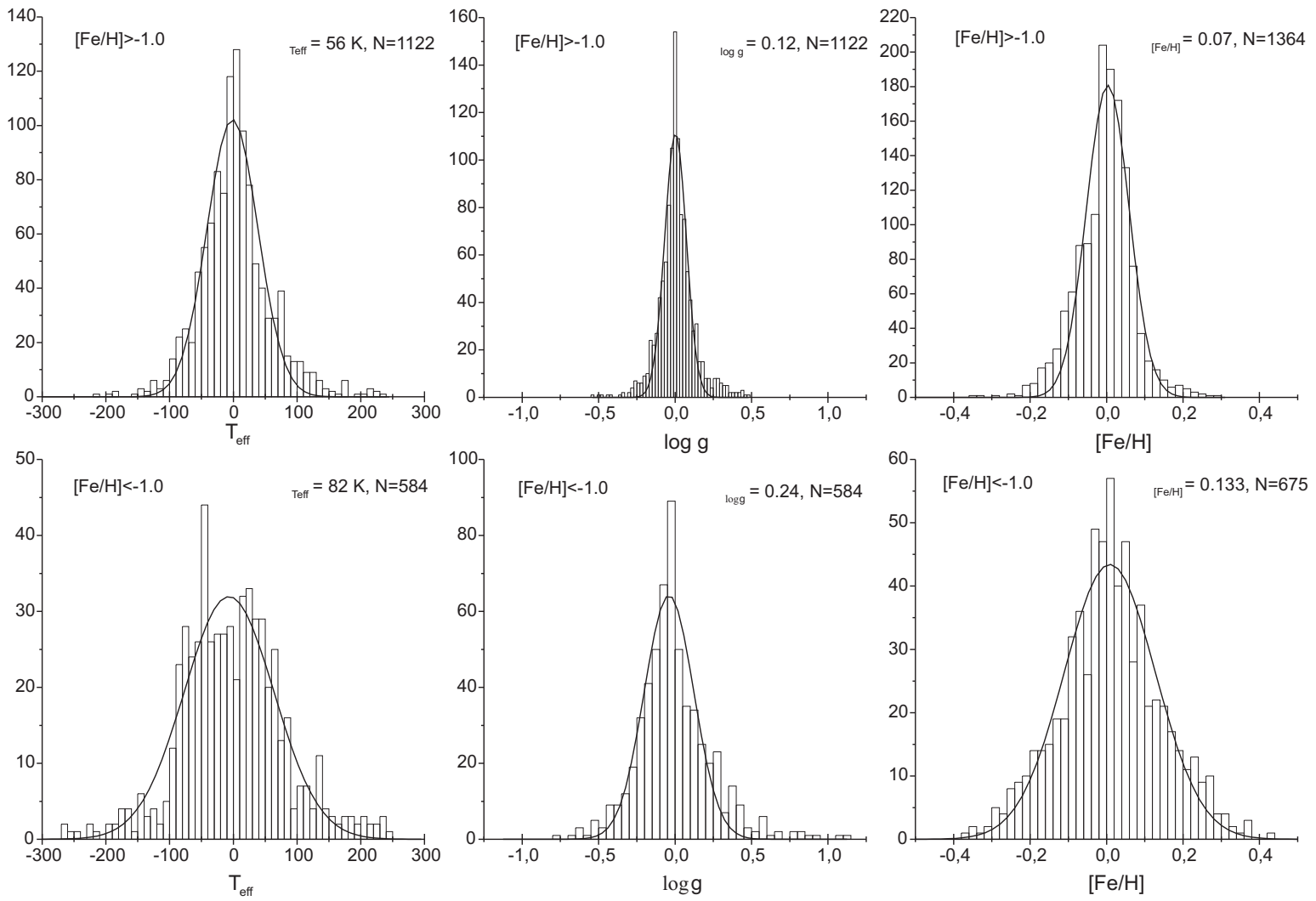


Figure 2: The distribution of deviations of individual determinations of T_{eff} , $\log g$, and $[\text{Fe}/\text{H}]$ from the computed mean values. The upper row of the graphs is for the stars with $[\text{Fe}/\text{H}] > -0.1$, and the lower row, for $[\text{Fe}/\text{H}] < -1.0$. The curves approximate the distributions with a normal law. Dispersions and star numbers are indicated for the histograms.

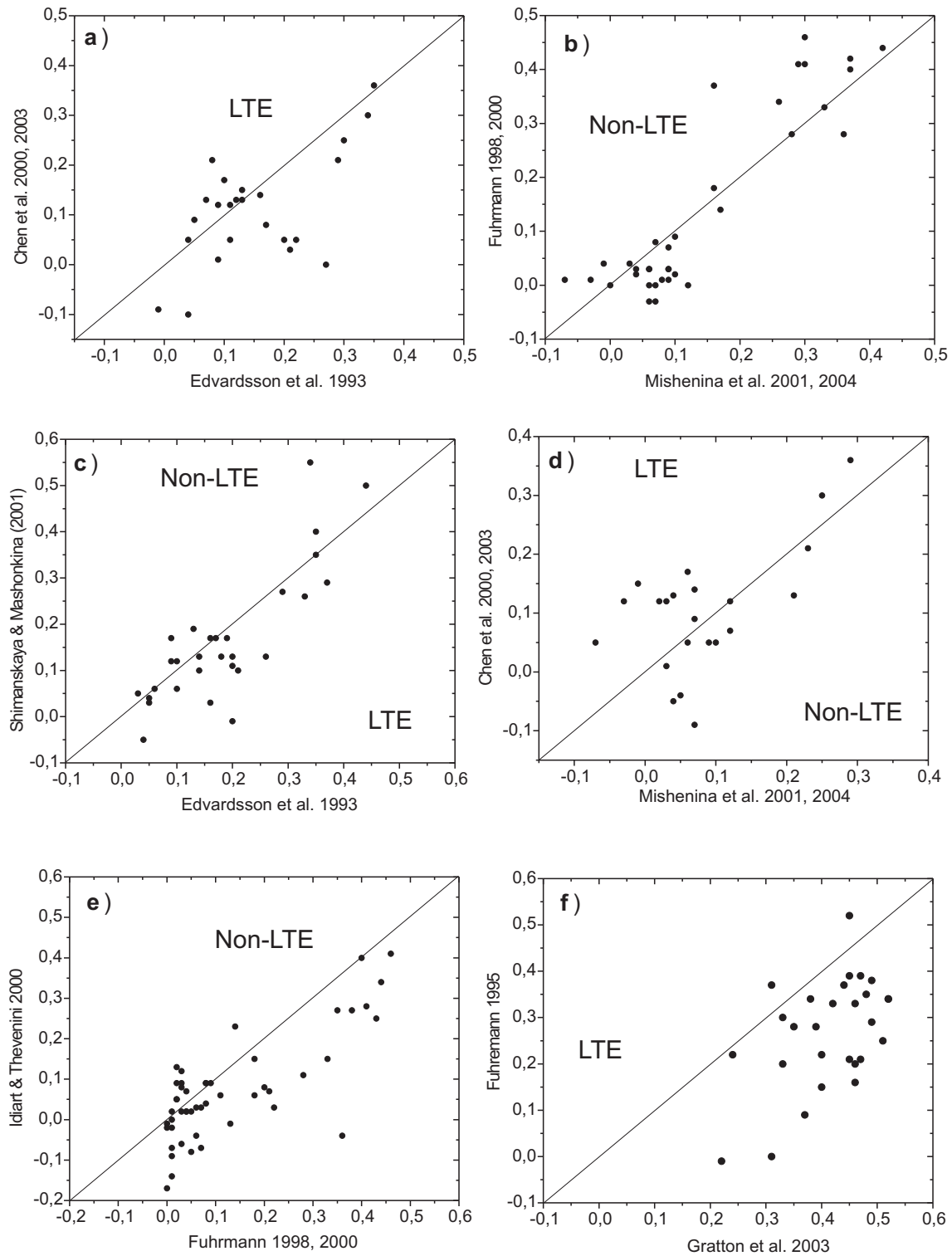


Figure 3: Comparison of [Mg/Fe] values from several authors. The approximation used by the corresponding authors for magnesium-abundance determinations is indicated.

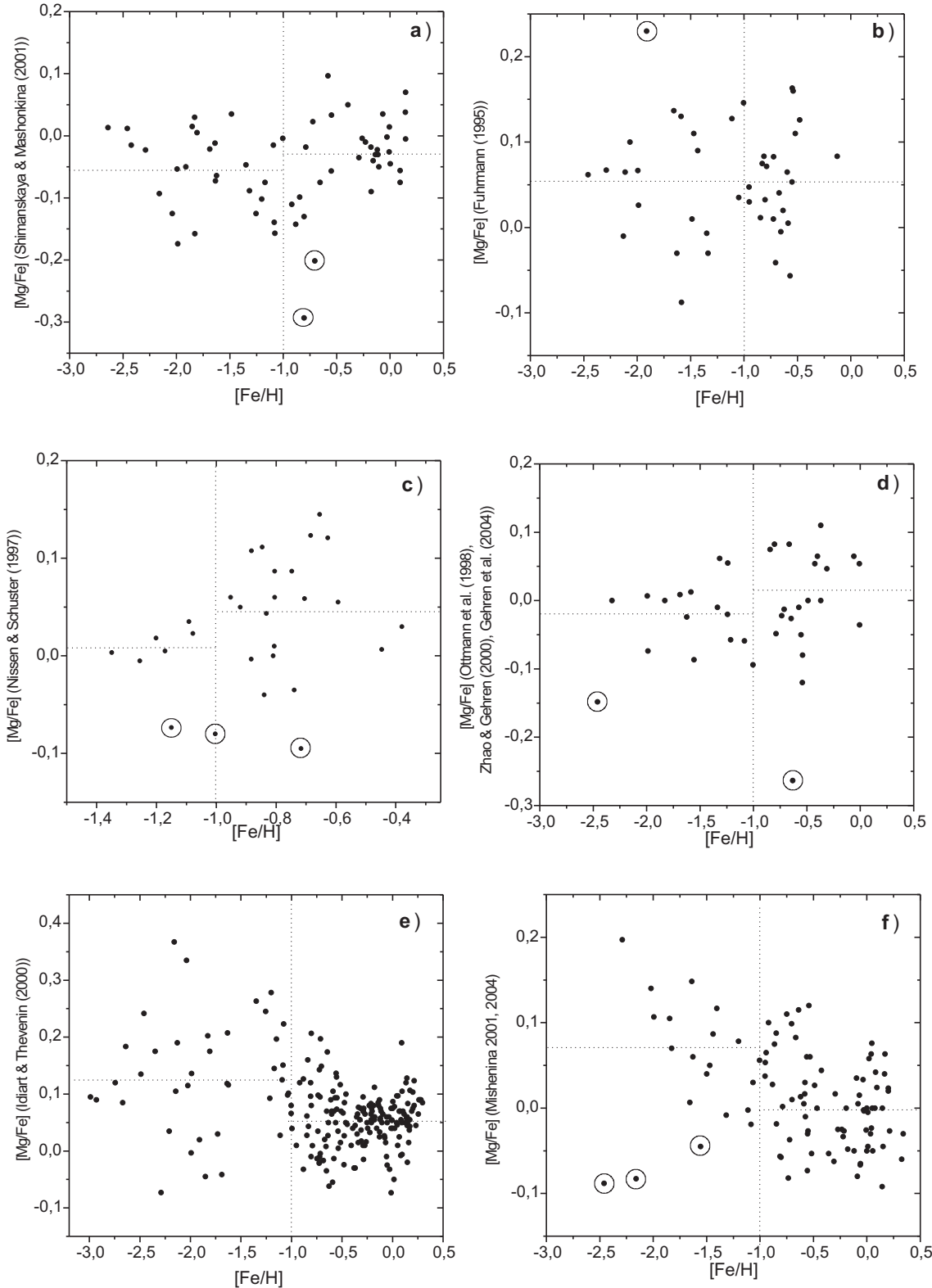


Figure 4: The relation between metallicities and deviations of individual magnesium-abundance determinations (from several sources) from those computed as averages from all the authors, ($\delta[Mg/Fe]$). The values rejected using the 3σ criterion in the scatter ($\sigma_{\delta[Mg/Fe]}$) or deviation ($\Delta[Mg/Fe]_j$) computations are circled. The horizontal lines are mean deviations for each of the ranges.

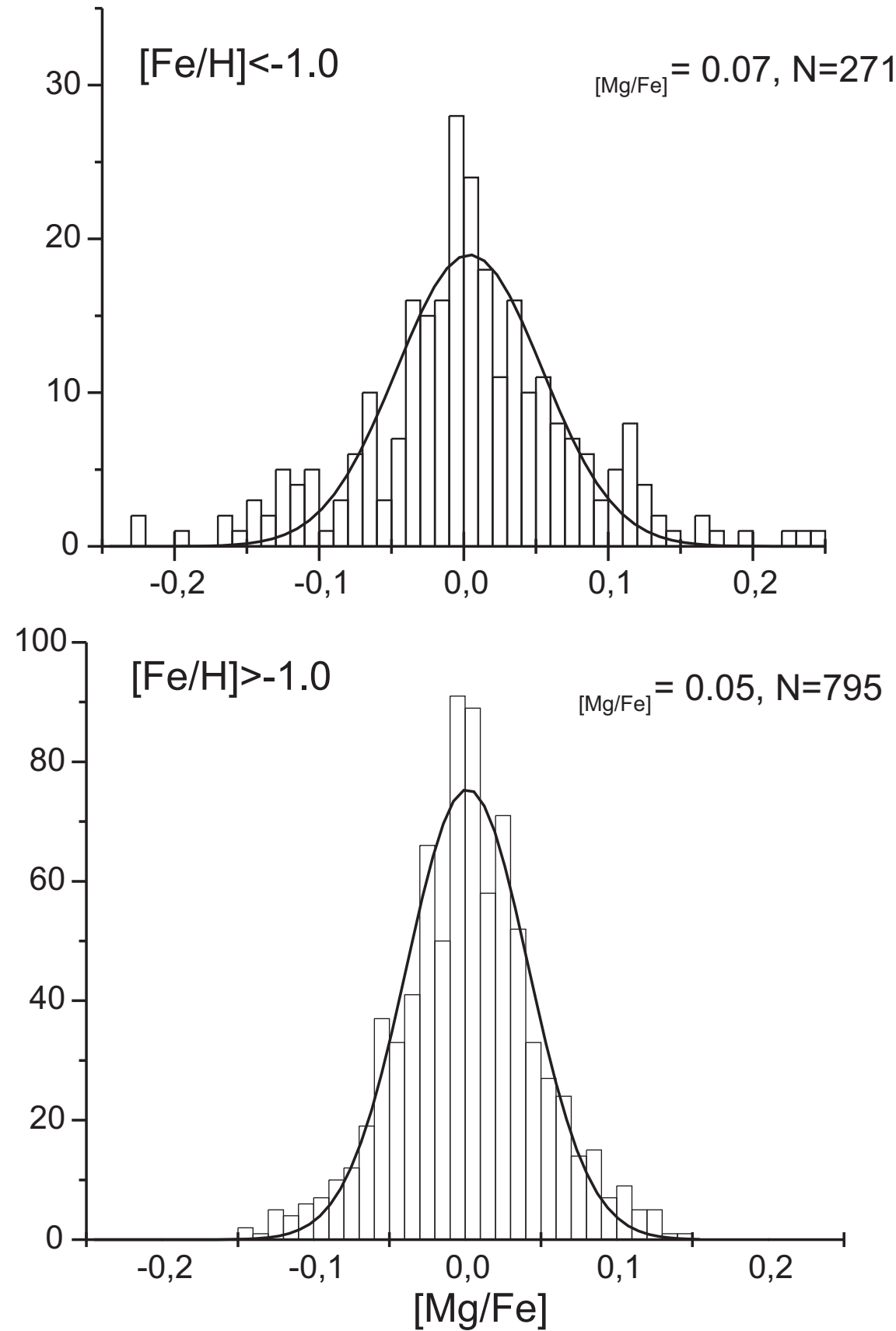


Figure 5: The distributions of the $\delta[\text{Mg}/\text{Fe}]$ deviations for the two metallicity ranges. The notation is as in Fig. 2.

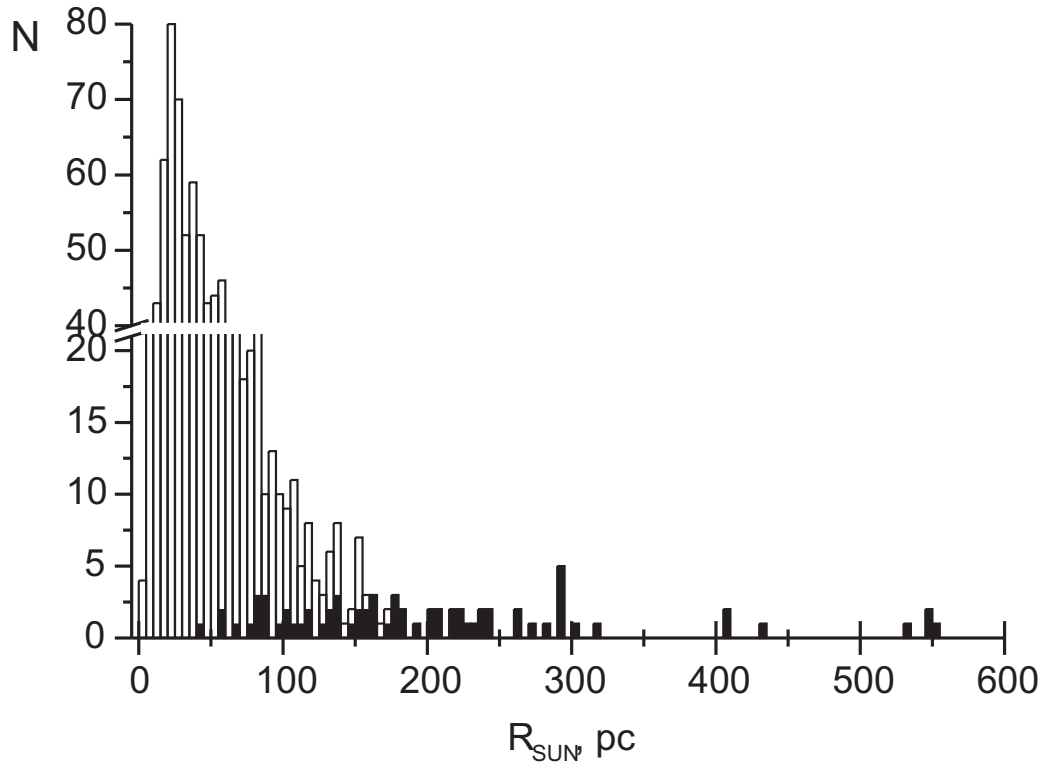


Figure 6: The distribution of the distance of the catalog stars from the Sun derived from trigonometric parallaxes (open bars) and from photometric measurements (filled bars).

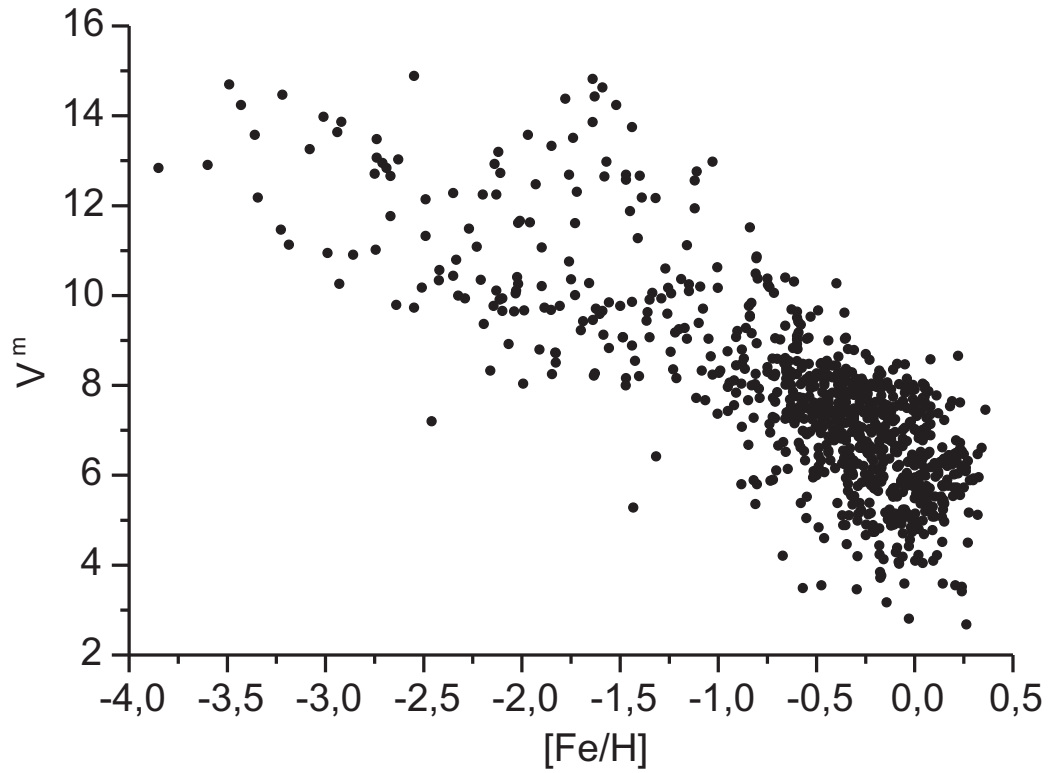


Figure 7: The metallicity versus apparent magnitude.

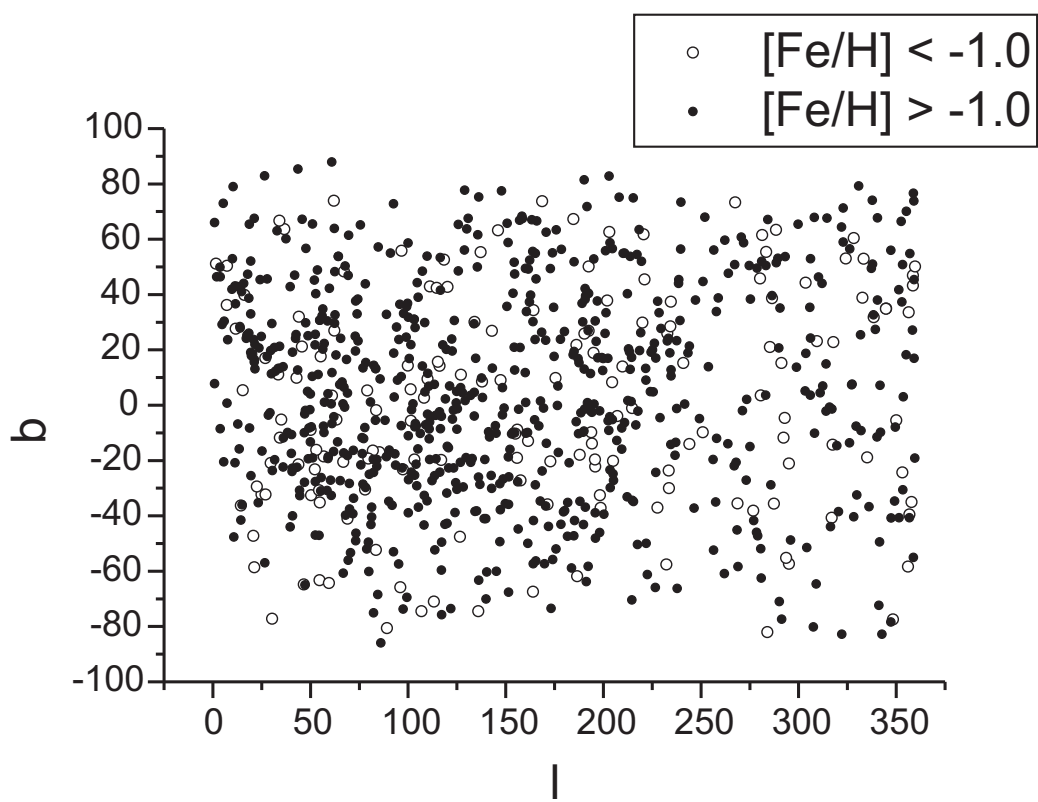


Figure 8: Positions of metal-rich (filled circles) and metal-poor (open circles) stars on the sky.

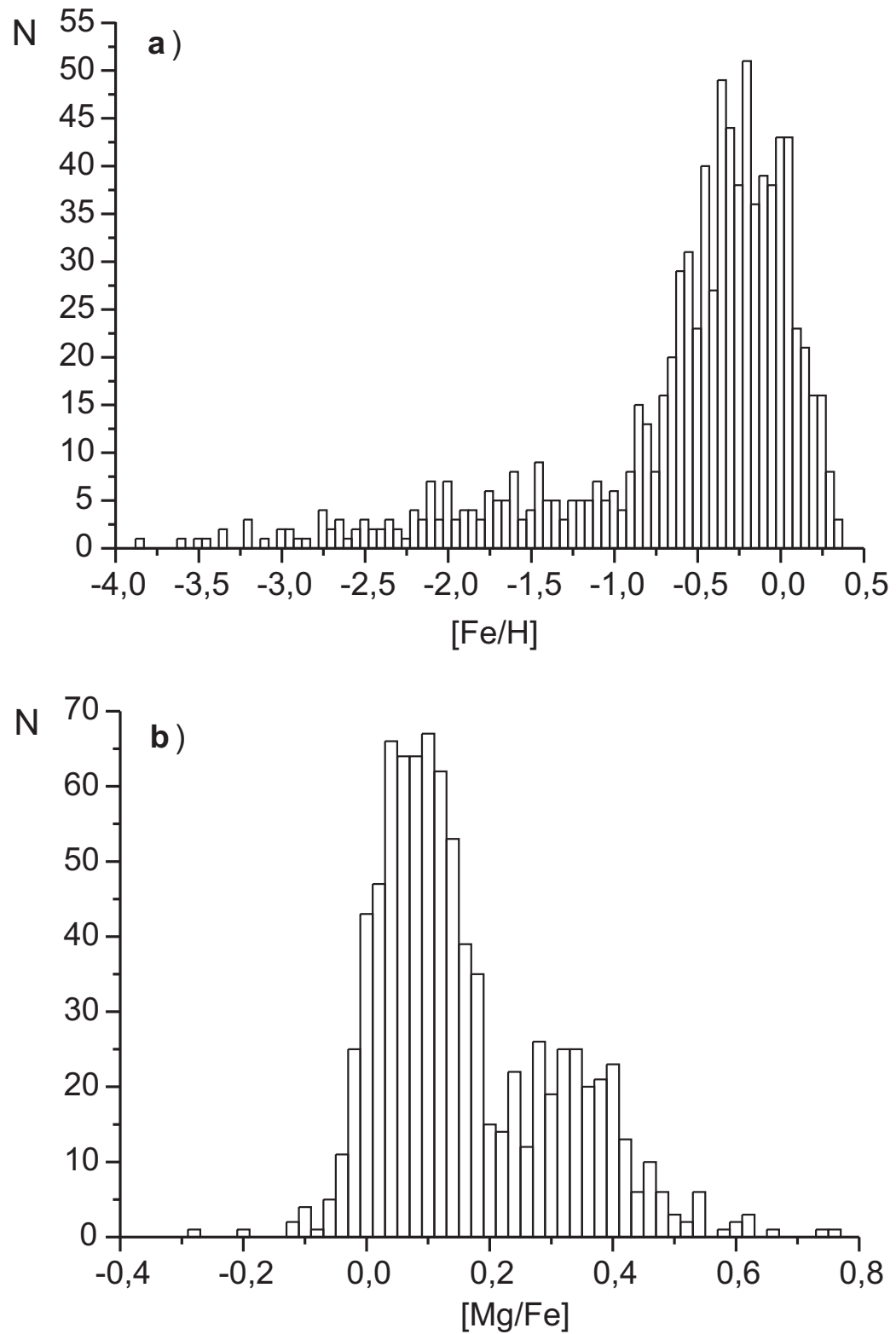


Figure 9: The distributions of the (a) iron abundance and (b) relative magnesium abundances of the catalog stars.

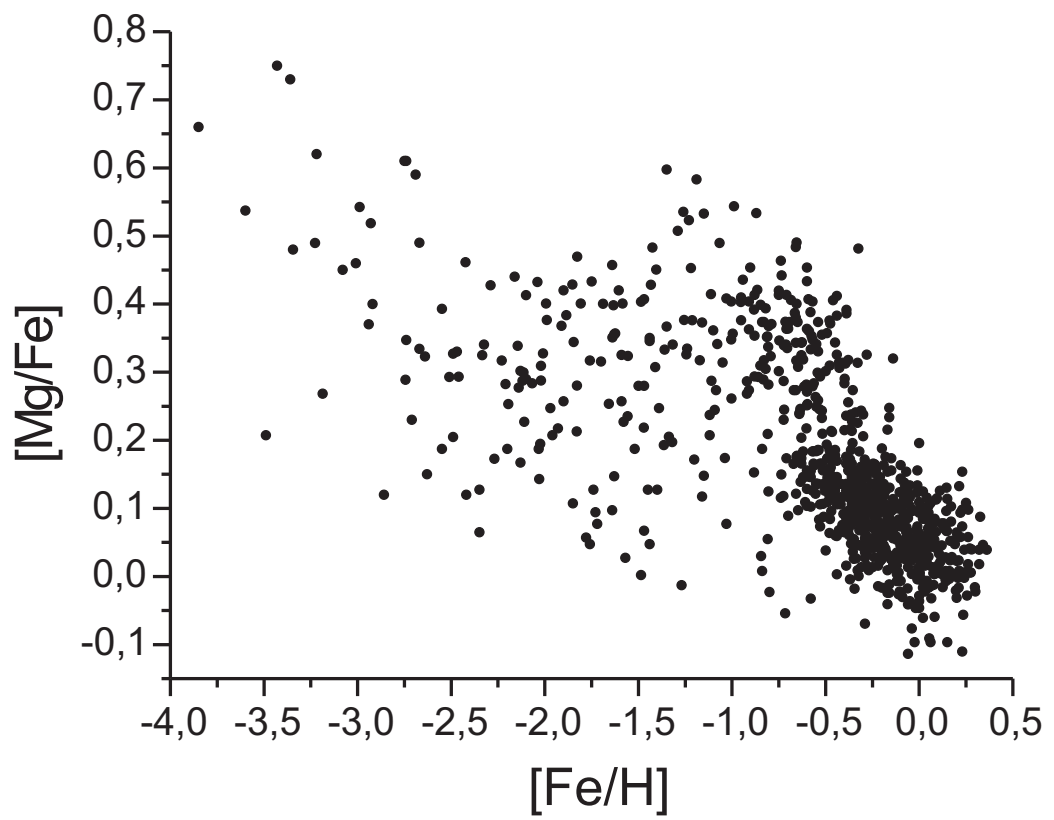


Figure 10: The metallicity versus magnesium abundance for the catalog stars stars.